RAA 2016 Vol. 16 No. 5, 83 (8pp) doi: 10.1088/1674–4527/16/5/083
http://www.raa-journal.org *http://iopscience.iop.org/raa*

Research in Astronomy and Astrophysics

Strong screening effects on resonant nuclear reaction ^{23}Mg (p, γ) ^{24}Al in the surface of magnetars

Jing-Jing Liu

College of Electronic and Communication Engineering, Hainan Tropical Ocean University, Sanya 572022, China; *liujingjing68@126.com*
Department of Astronomy and Institute of Theoretical Physics and Astrophysics, Xiamen University, Xiamen 361005, China

Received 2015 October 11; accepted 2016 February 1

Abstract Based on the theory of relativistic superstrong magnetic fields (SMFs), by using the method of Thomas-Fermi-Dirac approximations, we investigate the problem of strong electron screening (SES) in SMFs and the influence of SES on the nuclear reaction of ^{23}Mg $(p, \gamma)^{24}$Al. Our calculations show that the nuclear reaction will be markedly effected by the SES in SMFs in the surface of magnetars. Our calculated screening rates can increase two orders of magnitude due to SES in SMFs.

Key words: physical data and processes: nuclear reactions, nucleosynthesis, abundances — stars: neutron — stars: magnetic fields

1 INTRODUCTION

According to stellar evolution theory, for sufficiently high temperature in the Ne-Na cycle, the timescale of the proton capture reaction of ^{23}Mg is shorter than that of β^+-decay. Therefore, some ^{23}Mg will kindle and escape from the Ne-Na cycle by proton capture. The ^{23}Mg leaks from the Ne-Na cycle into the Mg-Al cycle and results in the synthesis of a large amount of heavy nuclei. Thus the reaction rate of ^{23}Mg (p, γ) ^{24}Al in the stellar environment is of great importance to nucleosynthesis of heavy nuclei. Due to its significance in astrophysical surroundings, the nuclear reaction rate of ^{23}Mg (p, γ) ^{24}Al has been extensively studied. For instance, by considering the contribution of a single resonance energy state, Wallace & Woosley (1981) first discussed the reaction rate of ^{23}Mg (p, γ) ^{24}Al. Based on the three resonances and a contribution from the direct capture process, Iliadis et al. (2001) investigated these nuclear reaction rates. Taking into account four resonances and the structure of ^{24}Al, Kubono et al. (1995) reconsidered the rate. Other authors (e.g., Herndl et al. 1998; Visser et al. 2007; Lotay et al. 2008) also carried out estimations for the rate based on some new experimental information on ^{24}Al excitation energies. However, these authors seem to have overlooked one important influence of electron screening on the nuclear reaction in a superstrong magnetic field (SMF).

Strong electron screening (SES) has always been a challenging problem in stellar weak-interaction rates and thermonuclear reaction rates in pre-supernova stellar evolution and nucleosynthesis. Some works (e.g., Bahcall et al. 2002; Liu 2013a,b,c, 2014a,b, 2015) have been done on stellar weak-interaction rates and thermonuclear reaction rates. In a high-density plasma environment, the SES has been widely investigated by various screened Coulomb models, such as Salpeter's model (Salpeter 1954; Salpeter & van Horn 1969), Graboske's model (Graboske et al. 1973), and Dewitt's model (Dewitt 1976). Related discussions were provided by Liolios (2000), Liolios (2001) and Liu (2013c). Very recently, Spitaleri et al. (2015) also discussed electron screening and the nuclear clustering puzzle. Their results show that large values of screening potential are in fact due to clusterization effects in nuclear reactions, especially in reactions involving light nuclei. However, they neglected the effects of SES on the thermonuclear reaction rate in SMFs. How does the SES influence the nucleosynthesis and thermonuclear reactions in an SMF before a supernova explosion occurs? It is very interesting and challenging for us to understand the physical mechanism of SES in dense stars, especially magnetars.

Magnetars have been proposed to be peculiar neutron stars which could power their X-ray radiation by SMFs as high as $B \sim 10^{14} - 10^{15}$ G (e.g., Peng & Tong 2007; Gao et al. 2011a,b, 2012; Guo et al. 2015; Xu & Huang 2015; Xiong et al. 2016). Some extensive researches about the characteristics, emission properties, and the latest observations of magnetars have been done. These researches on the thermal and magnetic evolution of magnetars are very interesting and challenging tasks in astronomy and the astrophysical environment. For instance, Tong (2015) investigated the Galactic center magnetar SGR J1745−2900 and noted a puzzling spin-down behavior. Olausen & Kaspi (2014) presented a catalog of the 28 known magnetars and candidates. They investigated their observed thermal radiative properties in detail, and the quiescent X-ray emission. Szary et al. (2015) discussed some characteristics of radio emission from magnetars. Based on the estimated ages of potentially associated supernova remnants (SNRs) of magnetars, Gao et al. (2016) discussed the values of the mean braking indices of eight magnetars with SNRs. If the measurements of the SNR ages are reliable, Gao et al. (2016) may provide an effective way to constrain the magnetars' braking indices.

Recently, Li et al. (2016) numerically simulated the electron fraction and electron Fermi energy in the interior of a common neutron star. The electron Fermi energy and nuclear reaction rates inside a magnetar will be substantially affected by SMFs (e.g., Gao et al. 2011c,d, 2013, 2015). In an extremely strong magnetic field ($B \gg B_{\rm cr}$, $B_{\rm cr} = \frac{m_{\rm e}^2 c^3}{e\hbar} = 4.414 \times 10^3$ G is the quantum critical magnetic field), the Landau column becomes a very long and very narrow cylinder along the magnetic field. How does the quantization of Landau levels truly change with SMFs? This is a very interesting issue for us to discuss. Gao et al. (2013, 2015) investigated the electron degeneracy pressure from relativistic electrons in detail, and discussed the quantization of Landau levels for electrons, and the equations of states (EoSs) due to the quantum electrodynamic (QED) effects for different matter systems by introducing the Dirac δ-function in SMFs. Their results showed that the stronger the magnetic field strength is, the higher the electron degeneracy pressure becomes, and magnetars could be more compact and massive manifestations of neutron stars due to the contribution of magnetic field energy.

In this paper, based on the SES theory in SMFs (Fushiki et al. 1989), we will estimate the influence on the electron Fermi energy, the SES and change in electron energy due to SMFs, and discuss the influence on the thermonuclear reaction by SES in the surface of magnetars. Our work differs from previous works (e.g., Peng & Tong 2007; Gao et al. 2013, 2015) that discuss the electron Fermi energy in SMFs. Their works are based on the Pauli exclusion principle and Dirac δ-function in SMFs and investigate the influence of SMFs on the electron Fermi energy and electron pressure. Although they discussed the magnetic effects in detail, they seemed to lose sight of the influence of SMFs on SES. Following the works of Fushiki et al. (1989), we will reinvestigate the electron Fermi energy in SMFs, and derive new results for SES theory and screening rates for a nuclear reaction in SMFs, based on the Thomas-Fermi-Dirac (TFD) approximations. Secondly, our discussions also differ from those of Spitaleri et al. (2015), who analyzed the influence of the SES only in the case without SMFs. Finally, Potekhin & Chabrier (2013) also discussed the electron screening effect on stellar thermonuclear fusion. However, they just studied the impact of plasma correlation effects on nonresonant thermonuclear reactions in the liquid envelopes of neutron stars, and neglected the influence of SES on resonant nuclear rates in SMFs.

The article is organized as follows. In the next section, we will discuss the properties of the free electron gas including the electron Fermi energy and electron pressure in SMFs. Some expressions for the SES in an SMF will be given in Section 3. In Section 4, we will investigate the resonant reaction process and rates in the case with and without SES and SMFs. In Section 5, we will provide our main results and some discussions. Section 6 gives brief concluding remarks.

2 THE PROPERTIES OF THE FREE ELECTRON GAS IN AN SMF

Theoretical studies of matter in high magnetic fields have been carried out using a variety of methods, among which the Thomas-Fermi (TF) and TFD approximations are the most used methods, due to their simplicity but adequacy for many purposes. The TF method is the oldest and simplest case of a density functional theory. The total energy of a system of electrons and nuclei is written as a function of electron density. Detailed descriptions about the methods of TF and TFD approximations can be referenced in Fushiki et al. (1991, 1992).

The positive electron energy levels, including the contributions of spin while neglecting radiative corrections in SMFs, are given by (Landau & Lifshitz 1977)

$$E_n = n\hbar\omega_c + \frac{p_z^2}{2m_e}, \tag{1}$$

where $n = 0, 1, 2, ...$, $\hbar\omega_c = eB\hbar/m_e c \doteq 11.5 B_{12}$ keV is the electron cyclotron energy, B_{12} is the magnetic field in units of 10^{12}G, $p_{\rm z}$ is the electron momentum along the z-direction, and $m_{\rm e}$ is the electron mass. The electron chemical potential $U_{\rm e}$ is determined by inverting the expression for electron number density

$$n_{\rm e} = \left(\frac{eB}{hc}\right)\frac{2}{h}\left[p_{\rm F}(0) + 2\sum_{n=0}^{\infty} p_{\rm F}(n) H(U_{\rm e} - n\hbar\omega_c)\right], \tag{2}$$

where $p_{\rm F}(n) = [2m_{\rm e}(U_{\rm e} - n\hbar\omega_c)]^{1/2}$ is the maximum momentum along the z-direction for the $n-th$ Landau orbit and $H(x)$ is the Heaviside function, which is unity when x is positive and is zero otherwise. By integrating Equation (2) with respect to $U_{\rm e}$, and employing the Gibbs-Duhem equation, the pressure of electrons is written as

$$P = \left(\frac{eB}{hc}\right)\frac{2}{h}\left[\frac{p_{\rm F}^3(0)}{3m_{\rm e}} + 2\sum_{n=1}^{\infty}\frac{p_{\rm F}^3(n)}{3m_{\rm e}}H(U_{\rm e} - n\hbar\omega_c)\right]. \tag{3}$$

By summing over n, and integrating Equation (1), the total kinetic energy density, including contributions from the Landau orbital motion perpendicular to the field, the motion along the field and the coupling of the electron spin to the field, is

$$E_{\rm kin} = \left(\frac{eB}{hc}\right)\frac{2}{h}\left\{\frac{p_{\rm F}^3(0)}{6m_{\rm e}} + 2\sum_{n=1}^{\infty}\left[\frac{p_{\rm F}^3(n)}{6m_{\rm e}} + n\hbar\omega_c p_{\rm F}(n)\right]H(U_{\rm e} - n\hbar\omega_c)\right\}. \tag{4}$$

According to the TFD approximations, the electron energy density will include the contribution of electron exchange energy, and is given by (Danz & Glasser 1971)

$$E_{\rm ex} = \frac{e^2}{2}\left(\frac{eB}{hc}\right)^{-1} n_{\rm e}^2 F\left(\frac{n_{\rm e}}{n_*}\right) = \frac{r_{\rm cyc}}{2\pi a_0}\hbar\omega_c n_* n^2 F(n), \tag{5}$$

where $a_0 = 5.29\times10^9$ cm is the Bohr radius, $n_* = 2/\pi^{1/2}(eB/hc)^{3/2} = 4.24\times10^{27}B_{12}^{3/2}{\rm cm}^{-3}$, B_{12} is the magnetic field in units of 10^{12} G, and $r_{\rm cyc} = (2\hbar c/eB)^{1/2} \doteq 3.63\times10^{10}$ cm is the electron cyclotron radius in the lowest Landau level.

From the TFD approximations, when only a single Landau level is occupied, the electron chemical potential, which includes the contribution of electron exchange energy, is determined by

$$U_e = \frac{\partial E_{\rm ex}}{\partial n_{\rm e}} = e^2\left(\frac{eB}{hc}\right)^{-1} n_{\rm e} I\left(\frac{n_{\rm e}}{n_*}\right) = \frac{r_{\rm cyc}}{\pi a_0}\hbar\omega_c n_* n I(n), \tag{6}$$

where the expression of function $F(n)$ can be referenced in Fushiki et al. (1989).

According to Equation (1), the electron interaction energy with the magnetic field is proportional to the quantum number n, and cannot exceed the electron chemical potential. Thus the maximum number of Landau levels $n_{\rm max}$ will be related to the highest value of interaction energy allowed between electrons and the external magnetic field. When $E(n_{\rm max}, p_z = 0) = U_{\rm e}$ in Equation (1), the maximum number of Landau levels $n_{\rm max}$ will be given by

$$n_{\rm max} = \frac{U_{\rm e}}{\hbar\omega_c}. \tag{7}$$

In the general case, when $0 \le n \le n_{\rm max}$, the electron momentum is less than its Fermi momentum $p_{\rm F}(e)$, which is determined by

$$p_{\rm F}(e) = U_{\rm e}/c, \tag{8}$$

when $n = 0$ for an SMF (e.g., Gao et al. 2013, 2015).

3 THE SES IN AN SMF

According to Fushiki et al. (1989), the nuclear reaction rate in high-density matter is affected because the clouds of electrons around nuclei alter the interactions among nuclei. Due to the electron clouds, the reaction rate is increased by a factor of e^{U_{sc}/k_BT}, where U_{sc} is a negative quantity, called “the screening potential,” and T is the temperature. The electron Coulomb energy is described by the Wigner-Seitz approximation in an SMF as

$$U_{\rm sc} = E_{\rm atm}(z_{12}) - E_{\rm atm}(z_1) - E_{\rm atm}(z_2), \tag{9}$$

where $E_{\rm atm}(z)$ is the total energy of the Wigner-Seitz cell and $z_{12} = z_1 + z_2$. If the electron distribution is rigid, the contribution to $E_{\rm atm}(z)$ from the bulk electron energy cancels and the electron screening potential (ESP) at high density can be expressed as

$$U_{\rm sc} = E_{\rm latt}(z_{12}) - E_{\rm latt}(z_1) - E_{\rm latt}(z_2) = \frac{-0.9e^2}{r_{\rm e}}\left[z_{12}^{5/3} - z_1^{5/3} - z_2^{5/3}\right], \tag{10}$$

where $E_{\rm latt}(z)$ is the electrostatic energy of the Wigner-Seitz cell, $E_{\rm atm}(z_j) = \frac{-0.9 z_j^{5/3} e^2}{r_{\rm e}}$, and $r_{\rm e}$ is the radius of the Wigner-Seitz cell for a single electron. Due to the influence of the compressibility of electron gas, the change in screening potential is written as

$$\begin{aligned}\delta U_{\rm s} &= -\frac{54}{175}\left(\frac{e^2}{r_{\rm e}}\right)\frac{1}{n_{\rm e}}\frac{\partial n_{\rm e}}{\partial U_{\rm e}} \times \left[(z_{12})^{7/3} - (z_1)^{7/3} - (z_2)^{7/3}\right] \\ &= -\frac{54}{175}\left(\frac{e^2}{r_{\rm e}}\right)\frac{1}{n_{\rm e}} D \times \left[(z_{12})^{7/3} - (z_1)^{7/3} - (z_2)^{7/3}\right],\end{aligned} \tag{11}$$

where

$$D = 823.1481 \frac{r_{\rm e} n_{\rm e}}{e^2}\left(\frac{\overline{A}}{z}\right)^{4/3} \rho^{-4/3} B_{12}^2. \tag{12}$$

The TF screening wavenumber will be given by

$$(K_{\rm TF})^2 = 1.0344 \times 10^4 r_{\rm e} n_{\rm e}\left(\frac{\overline{A}}{z}\right)^{4/3} \rho^{-4/3} B_{12}^2. \tag{13}$$

According to Fushiki et al. (1989), the corresponding change of screening potential in an SMF is

$$\begin{aligned}\delta U_{\rm s} &= -0.254\left(\frac{\overline{A}}{z}\right)^{4/3} \rho^{-4/3} B_{12}^2 \times \left[(z_{12})^{7/3} - (z_1)^{7/3} - (z_2)^{7/3}\right] \\ &= -494.668\left(\frac{\overline{A}}{z}\right)^{4/3} \rho^{-4/3} b^2 \times \left[(z_{12})^{7/3} - (z_1)^{7/3} - (z_2)^{7/3}\right] \text{MeV},\end{aligned} \tag{14}$$

where $\left(\frac{\overline{A}}{z}\right)$ is the average $\frac{A}{z}$ ratio, corresponding to the mean molecular weight per electron, and $b = B/B_{\rm cr} = 0.02266 B_{12}$. Thus, the ESP in SMFs of the FGP model is given by

$$U_{\rm s} = U_{\rm sc} + \delta U_{\rm s}. \tag{15}$$

4 THE RESONANT REACTION PROCESS AND RATES

4.1 The Calculation of Resonant Reaction Rates with and without SES

The reaction rates are contributed from the resonant and non-resonant reactions. In the case of a narrow resonance, the resonant cross section σ_r is approximated by a Breit-Wigner expression (Fowler et al. 1967)

$$\sigma_{\rm r}(E) = \frac{\pi\omega}{\kappa^2}\frac{\Lambda_i(E)\Lambda_f(E)}{(E - E_{\rm r}^2) + \frac{\Lambda_{\rm tot}^2(E)}{4}}, \tag{16}$$

where κ is the wave number, and the entrance and exit channel partial widths are $\Lambda_i(E)$ and $\Lambda_f(E)$, respectively, $\Lambda_{\rm tot}(E)$ is the total width and ω is a statistical factor which is given by

$$\omega = (1 + \delta_{12})\frac{2J + 1}{(2J_1 + 1)(2J_2 + 1)}, \tag{17}$$

where the spins of the interacting nuclei and resonance are J_1 and J_2, respectively, and δ_{12} is the Kronecker delta function.

The partial widths depend on the energy and can be expressed as (Lane & Thomas 1958)

$$\Lambda_{i,f} = 2\vartheta_{i,f}^2 \psi_l(E, a) = \Lambda_{i,f}\frac{\psi_l(E, a)}{\psi_l(E_f, a)}. \tag{18}$$

The penetration factor ψ_l is associated with l and a, which are the relative angular momentum and the channel radius, respectively; a is written as $a = 1.4(A_1^{1/3} + A_2^{1/3})$ fm. $\Lambda_{i,f}$ is the partial energy width at the resonance process. $\vartheta_{i,f}^2$ is the reduced width and given by

$$\vartheta_{i,f}^2 = 0.01\vartheta_{\rm w}^2 = \frac{0.03\hbar^2}{2Aa^2}. \tag{19}$$

Based on the above, in the phases of explosive stellar burning, the narrow resonance reaction rates without SES are determined by (Schatz et al. 1998; Herndl et al. 1998)

$$\lambda_{\rm r}^0 = N_{\rm A}\langle\sigma v\rangle_{\rm r} = 1.54 \times 10^{11}(AT_9)^{-3/2}\sum_i \omega\gamma_i \exp(-11.605 E_{r_i}/T_9)\,\text{cm}^3\,\text{mol}^{-1}\,\text{s}^{-1}, \tag{20}$$

where $N_{\rm A}$ is Avogadro's constant, A is the reduced mass of the two collision partners, E_{r_i} is the resonance energies and T_9 is the temperature in units of 10^9 K. $\omega\gamma_i$ is the resonance strength in units of MeV and is determined by

$$\omega\gamma_i = (1+\delta_{12})\frac{2J+1}{(2J_1+1)(2J_2+1)}\frac{\Lambda_i\Lambda_f}{\Lambda_{\rm total}}. \tag{21}$$

On the other hand, due to SES, the reaction rates of a narrow resonance are given by

$$\begin{aligned}\lambda_{\rm r}^s &= F_{\rm r}N_{\rm A}\langle\sigma v\rangle_{\rm r'} = 1.54\times10^{11}(AT_9)^{-3/2}\sum_i\omega\gamma_i\exp(-11.605E'_{r_i}/T_9)\\ &= 1.54\times10^{11}F_{\rm r}(AT_9)^{-3/2}\sum_i\omega\gamma_i\exp(-11.605E_{r_i}/T_9)\ \ {\rm cm^3\,mol^{-1}\,s^{-1}},\end{aligned} \tag{22}$$

where $F_{\rm r}$ is the screening enhancement factor (hereafter SEF). The values of ${E'}_{r_i}$ should be measured by experiments, but it is too hard to provide sufficient data. In a general and approximate analysis, we have ${E'}_{r_i} = E_{r_i} - U_0 = E_{r_i} - U_{\rm s}$.

4.2 The Screening Model of Resonant Reaction Rates in the Case with SMFs

It is widely known that nuclear reaction rates at low energies play a key role in energy generation in stars and stellar nucleosynthesis. The bare reaction rates are modified in stars by the screening effects of free and bound electrons. Knowledge about the bare nuclear reaction rates at low energies is important not only for understanding various astrophysical nuclear problems, but also for assessing the effects of host material in low energy nuclear fusion reactions in stellar matter.

As mentioned in Section 1, most magnetars possess superstrong surface dipole magnetic fields, and the internal magnetic field may be higher than the surface magnetic field (e.g., Peng & Tong 2007). Since the Fermi energy of the electron gas may go up to 10 MeV, the quantum effects of electron gas will be very obvious and sensitive to SMFs. The electron phase space will be strongly modified by SMFs. Electron screening will play a key role in this process. It can strongly effect the electron transformation and nuclear reaction rates. In this subsection, we will discuss the screening potential in the strong screening limit. The dimensionless parameter (Γ), which determines whether or not correlations between two species of nuclei (z_1, z_2) are important, is given by

$$\Gamma = \frac{z_1z_2e^2}{(z_1^{1/3}+z_2^{1/3})r_{\rm e}kT}. \tag{23}$$

Under the condition of $\Gamma \gg 1$, the nuclear reaction rates will be influenced appreciably by SES. The SEF for the resonant reaction process in SMFs can be expressed as

$$F_{\rm r}^{\rm B} = \exp\left(\frac{11.605U_{\rm s}}{T_9}\right). \tag{24}$$

5 RESULTS AND DISCUSSIONS

According to the electron screening model of Fushiki et al. (1989) in SMFs, we have calculated the electron screening potential at different temperatures from Equations (10), (14) and (15), based on the TFD approximations.

Figure 1 shows that the ESP is a function of B_{12}. We found that the SMFs have a slight influence on the ESP in the high-density surroundings (e.g., $\rho_7 \geq 1.3$), but the influence on ESP is very remarkable for relatively low densities (e.g., $\rho_7 = 0.1, 0.3, 0.5$) in SMFs. Due to the fact that the higher the density is, the larger the electron energy becomes, it will definitely blunt the impact of SMFs on ESP. For example, the ESP increases greatly when $B_{12} < 10^3$, and will reach the maximum value of 0.0188 MeV when $B_{12} = 580.7$ and $\rho_7 = 0.1$. However, the ESP decreases about two orders of magnitude when $10^3 < B_{12} < 2\times10^3$ and $\rho_7 = 0.1$.

The influence of SES in SMFs on a nuclear reaction is mainly reflected by the factor of SEF. According to Equations (22), (24) and some parameters of Table 1, we have calculated and analyzed the factor of SEF in detail.

Figure 2 demonstrates that the SEF is a function of magnetic field strength B for different temperature-density surroundings. We find that the influences of SES on SEF are very remarkable in SMFs. The lower the temperature is, the greater the influence on SEF becomes. This is because the electron kinetic energy is relatively low at lower temperatures. With the increase of magnetic field strength B, the SEF decreases. On the contrary, the SEF greatly increases with increasing B at relatively high densities (e.g., $\rho_7 = 1.0$).

Table 2 shows some important information about the SEF at certain astronomical conditions. We find that the lower the temperature, the greater the influence on the SEF. With increasing temperature at the same density, the maximum value of SEF decreases. The maximum value of SEF will be 3289 when $B_{12} = 10^3, \rho_7 = 10$ and $T_9 = 0.1$. This is due to the fact that the higher the temperature increases, the larger the electron energy becomes. According to Equations (20) and (22), we can see that the nuclear reaction rates will increase as temperature increases.

It is well known that, in stellar environments where explosive hydrogen burning occurs, the nuclear reaction $^{23}{\rm Mg}(p,\gamma)^{24}{\rm Al}$ plays a key role in breaking out of the Ne-Na cycle to heavier nuclear species (e.g., the Mg-Al cycle). Therefore, it is very important to accurately determine the rates for the reaction $^{23}{\rm Mg}(p,\gamma)^{24}{\rm Al}$. However, the

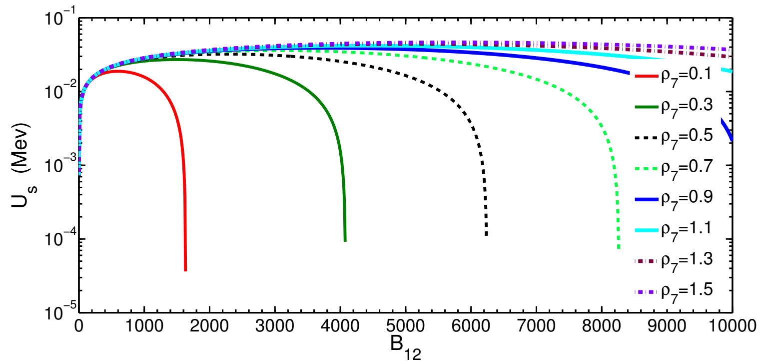

Fig. 1 The ESP as a function of B under certain astronomical conditions.

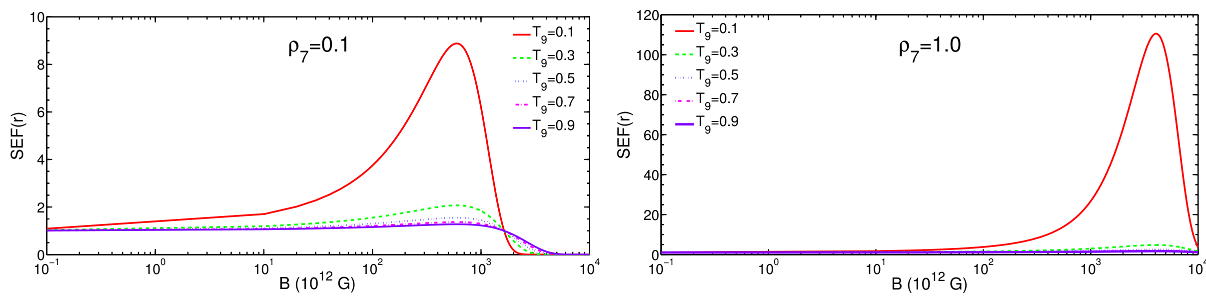

Fig. 2 The SEF as a function of B for $\rho_7 = 0.1$ (*left*) and 1.0 (*right*) under certain astronomical conditions.

Table 1 Resonance Parameters for the Reaction ^{23}Mg (p,γ) ^{24} Al

E_x (MeV) [1]	E_x (MeV)[2]	J^π	E_{r_i} (MeV) [3]	Γ_p	Γ_γ	$\omega\gamma_i$ (MeV) [4]	$\omega\gamma_i$ (MeV) [5]	$\omega\gamma_i$ (MeV) [6]
2.349±0.020	2.346±0.000	3^+	0.478	185	33	25	27	26
2.534±0.013	2.524±0.002	4^+	0.663	2.5e3	53	58	130	94
2.810±0.020	2.792±0.004	2^+	0.939	9.5e5	83	52	11	31.5
2.900±0.020	2.874±0.002	3^+	1.029	3.4e4	14	12	16	14

Notes: [1] is adopted from Endt (1998); [2] from Visser et al. (2007); [3] from Audi & Wapstra (1995); [4] from Herndl et al. (1998); [5] from Wiescher et al. (1986); [6] is adopted in this paper.

Table 2 Maximum Value of the Strong SEF for Some Typical Astronomical Conditions

	$\rho_7 = 0.01$		$\rho_7 = 0.1$		$\rho_7 = 1.0$		$\rho_7 = 10$	
T_9	B_{12}	$\mathrm{SEF}_{\max}$	B_{12}	$\mathrm{SEF}_{\max}$	B_{12}	$\mathrm{SEF}_{\max}$	B_{12}	$\mathrm{SEF}_{\max}$
0.1	90.19	2.755	590.7	8.881	4074	110.5	1000	3289
0.3	90.19	1.402	610.7	2.071	3954	4.797	1000	1487
0.5	100.2	1.223	650.7	1.546	4074	2.563	1000	5.046
0.7	110.2	1.152	690.8	1.362	4204	1.985	1000	3.179
0.9	120.2	1.113	630.7	1.274	3914	1.686	1000	2.450

resonance energy has a large uncertainty due to inconsistent ^{24}Mg(^{3}He,t)^{24}Al measurements, as mentioned above. Since different evaluation methods may result in different orders for the reaction, the evenness method is adopted to increase the accuracy of the comprehensive evaluation of Table 1.

According to Equations (22), (24) and some parameters of Table 1, the resonant rates for four resonance states in the case with and without SES are functions of T_9, as shown in Figure 3. The results show that the contributions of four resonant states to the total reaction rate have an obvious difference at the stellar temperature range of $T_9 = 0.1 - 5$. With an increase of temperature, the rates increase quickly. One can find that the contribution of the resonance state of $E_r = 478$ keV dominates the total reaction rates when $T_9 = 0.2 - 1.681$, but the $E_r = 663$ keV resonance is the most important at high temperatures of $T_9 > 1.681$. On the contrary, the $E_r = 939$ keV as well as $E_r = 1029$ keV resonance states are negligible compared to the former two lower resonance states over the whole temperature range.

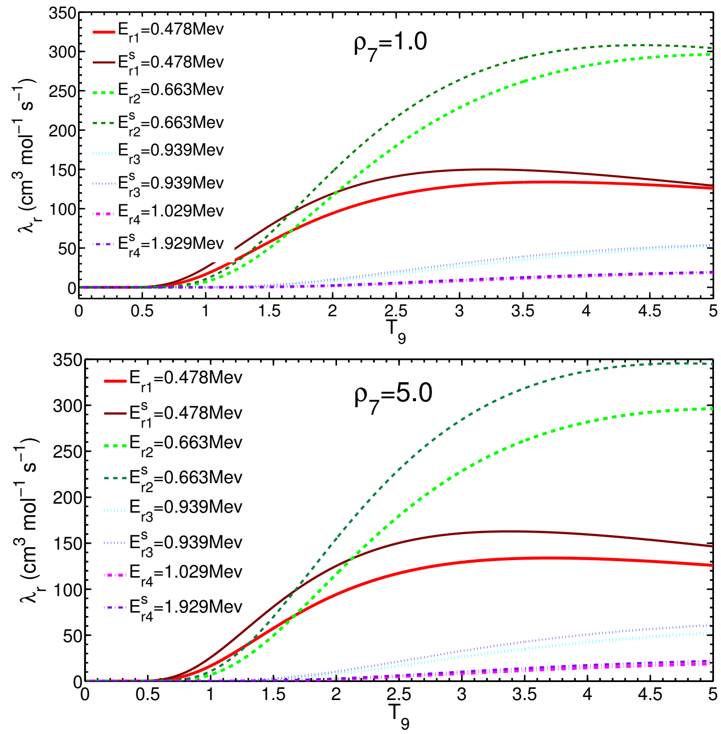

Fig. 3 The nuclear reaction rates in the case with and without SES as a function of T_9 for $\rho_7 = 1.0, 5.0$ and 10^3 G $\leq$ B $\leq 10^{16}$ G in different energy states.

Table 3 Maximum Value of Strong Screening Enhancement Rates for Some Typical Astronomical Conditions

	$\rho_7 = 1.0$		$\rho_7 = 5.0$		$\rho_7 = 10$		$\rho_7 = 100$	
E (MeV)	$\lambda^0_{\rm max}$	$\lambda^s_{\rm max}$	$\lambda^0_{\rm max}$	$\lambda^s_{\rm max}$	$\lambda^0_{\rm max}$	$\lambda^s_{\rm max}$	$\lambda^0_{\rm max}$	$\lambda^s_{\rm max}$
$E_1 = 0.478$	131.9	149.9	590.7	8.881	133.7	163.8	133.9	164.7
$E_2 = 0.663$	296.2	307.9	610.7	2.071	296.2	350.2	296.2	350.5
$E_3 = 0.939$	51.50	53.16	650.7	1.546	52.31	61.50	52.24	61.90
$E_4 = 1.929$	18.45	19.08	690.8	1.362	18.59	22.18	18.56	22.27

Table 3 gives a brief description of the resonant rates for four resonance states due to SES in SMFs. One can find that the maximum value of strong screening rates will reach 350.5 when $E_2 = 0.663$ MeV and $\rho_7 = 100$.

In summary, by analyzing the influence of SES on the resonant rates in SMFs, we find that the SES has different effects on the rates for different resonance states because of different forms of energy and reaction orbits in the process of reaction in SMFs. We show that this effect by SES is remarkable and can increase reaction rates by more than two orders of magnitude.

6 CONCLUDING REMARKS

The properties of matter in magnetars have always been interesting and challenging topics for astronomers and physicists. The investigation of SES is obviously an important component of magnetar research. In particular, improving the interpretation of nuclear reaction data by SES in magnetars requires a detailed theoretical understanding of physical properties for highly-magnetized nuclear matter.

In this paper, by employing the method of TFD approximations in SMFs, we have investigated the problem of SES, and the effects of SMFs on the nuclear reaction of ^{23}Mg $(p, \gamma)^{24}$Al. Our calculations showed that the nuclear reaction will be markedly affected by SES in SMFs of magnetars. The calculated reaction rates can increase by more than two orders of magnitude. The considerable increase of reaction rates for ^{23}Mg (p, γ) ^{24}Al implies that more ^{23}Mg will escape the Ne-Na cycle due to SES, which will make the next reaction convert more ^{24}Al (β^+, ν) ^{24}Mg to participate in the Mg-Al cycle. It may lead to synthesizing a large amount of heavy elements (e.g., ^{26}Al) within the outer crust of magnetars.

Acknowledgements We thank the anonymous referee for carefully reading the manuscript and providing valuable comments that improved this paper substantially. This work is supported in part by the National Natural Science Foundation of China through grant No. 11565020, the Natural Science Foundation of Hainan province under grant No. 114012, and the Undergraduate Innovation Program of Hainan province under grant No. 20130139.

References

Audi, G., & Wapstra, A. H. 1995, Nuclear Physics A, 595, 409

Bahcall, J. N., Brown, L. S., Gruzinov, A., & Sawyer, R. F. 2002, A&A, 383, 291

Danz, R. W., & Glasser, M. L. 1971, Phys. Rev. B, 4, 94

Dewitt, H. E. 1976, Phys. Rev. A, 14, 1290

Endt, P. M. 1998, Nuclear Physics A, 633, 1

Fowler, W. A., Caughlan, G. R., & Zimmerman, B. A. 1967, ARA&A, 5, 525

Fushiki, I., Gudmundsson, E. H., & Pethick, C. J. 1989, ApJ, 342, 958

Fushiki, I., Gudmundsson, E. H., Pethick, C. J., & Yngvason, J. 1991, Physics Letters A, 152, 96

Fushiki, I., Gudmundsson, E. H., Pethick, C. J., & Yngvason, J. 1992, Annals of Physics, 216, 29

Gao, Z. F., Peng, Q. H., Wang, N., Chou, C. K., & Huo, W. S. 2011a, Ap&SS, 336, 427

Gao, Z. F., Wang, N., Song, D. L., Yuan, J. P., & Chou, C.-K. 2011b, Ap&SS, 334, 281

Gao, Z. F., Wang, N., Yuan, J. P., et al. 2011c, Ap&SS, 333, 427

Gao, Z. F., Wang, N., Yuan, J. P., Jiang, L., & Song, D. L. 2011d, Ap&SS, 332, 129

Gao, Z. F., Peng, Q. H., Wang, N., & Yuan, J. P. 2012, Ap&SS, 342, 55

Gao, Z. F., Wang, N., Peng, Q. H., Li, X. D., & Du, Y. J. 2013, Modern Physics Letters A, 28, 1350138

Gao, Z. F., Wang, N., Xu, Y., Shan, H., & Li, X.-D. 2015, Astronomische Nachrichten, 336, 866

Gao, Z. F., Li, X.-D., Wang, N., et al. 2016, MNRAS, 456, 55

Graboske, H. C., Dewitt, H. E., Grossman, A. S., & Cooper, M. S. 1973, ApJ, 181, 457

Guo, Y.-J., Dai, S., Li, Z.-S., et al. 2015, RAA (Research in Astronomy and Astrophysics), 15, 525

Herndl, H., Fantini, M., Iliadis, C., Endt, P. M., & Oberhummer, H. 1998, Phys. Rev. C, 58, 1798

Iliadis, C., D'Auria, J. M., Starrfield, S., Thompson, W. J., & Wiescher, M. 2001, ApJS, 134, 151

Kubono, S., Kajino, T., & Kato, S. 1995, Nuclear Physics A, 588, 521

Landau, L. D., & Lifshitz, E. M. 1977, Quantum mechanics (3rd ed., Oxford: Pergamon Press)

Lane, A. M., & Thomas, R. G. 1958, Rev. Mod. Phys., 73, 629

Li, X. H., Gao, Z. F., Li, X. D., et al. 2016, International Journal of Modern Physics D, 25, 1650002

Liolios, T. E. 2000, European Physical Journal A, 9, 287

Liolios, T. E. 2001, Phys. Rev. C, 64, 018801

Liu, J.-J. 2013a, RAA (Research in Astronomy and Astrophysics), 13, 99

Liu, J.-J. 2013b, RAA (Research in Astronomy and Astrophysics), 13, 945

Liu, J.-J. 2013c, MNRAS, 433, 1108

Liu, J.-J. 2014a, RAA (Research in Astronomy and Astrophysics), 14, 971

Liu, J.-J. 2014b, MNRAS, 438, 930

Liu, J.-J. 2015, Ap&SS, 357, 93

Lotay, G., Woods, P. J., Seweryniak, D., et al. 2008, Phys. Rev. C, 77, 042802

Olausen, S. A., & Kaspi, V. M. 2014, ApJS, 212, 6

Peng, Q.-H., & Tong, H. 2007, MNRAS, 378, 159

Potekhin, A. Y., & Chabrier, G. 2013, Contributions to Plasma Physics, 53, 397

Salpeter, E. E. 1954, Australian Journal of Physics, 7, 373

Salpeter, E. E., & van Horn, H. M. 1969, ApJ, 155, 183

Schatz, H., Aprahamian, A., Goerres, J., et al. 1998, Phys. Rep., 294

Spitaleri, C., Bertulani, C. A., Fortunato, L., & Vitturi, A. 2015, arXiv:1503.05266

Szary, A., Melikidze, G. I., & Gil, J. 2015, ApJ, 800, 76

Tong, H. 2015, RAA (Research in Astronomy and Astrophysics), 15, 1467

Visser, D. W., Wrede, C., Caggiano, J. A., et al. 2007, Phys. Rev. C, 76, 065803

Wallace, R. K., & Woosley, S. E. 1981, ApJS, 45, 389

Wiescher, M., Gorres, J., Thielemann, F.-K., & Ritter, H. 1986, A&A, 160, 56

Xiong, X.-Y., Gao, C.-Y., & Xu, R.-X. 2016, RAA (Research in Astronomy and Astrophysics), 16, 009

Xu, M., & Huang, Y.-F. 2015, RAA (Research in Astronomy and Astrophysics), 15, 986